PHYSICAL REVIEW B **91**, 161104(R) (2015)

Jahn-Teller versus quantum effects in the spin-orbital material $LuVO_3$

M. Skoulatos,[1,2] S. Toth,[2] B. Roessli,[2] M. Enderle,[3] K. Habicht,[4] D. Sheptyakov,[2] A. Cervellino,[5] P. G. Freeman,[3,6] M. Reehuis,[4] A. Stunault,[3] G. J. McIntyre,[3] L. D. Tung,[7] C. Marjerrison,[8] E. Pomjakushina,[8] P. J. Brown,[3] D. I. Khomskii,[9] Ch. Rüegg,[2,10] A. Kreyssig,[11,12] A. I. Goldman,[11,12] and J. P. Goff[13]

[1]*Physik-Department, Technische Universität München, D-85748 Garching, Germany*
[2]*Laboratory for Neutron Scattering and Imaging, Paul Scherrer Institute, CH-5232 Villigen, Switzerland*
[3]*Institut Laue-Langevin, BP 156, F-38042 Grenoble Cédex 9, France*
[4]*Helmholtz-Zentrum Berlin für Materialien und Energie, Lise-Meitner-Campus, D-14109 Berlin, Germany*
[5]*Swiss Light Source, Paul Scherrer Institute, CH-5232 Villigen, Switzerland*
[6]*Laboratory of Quantum Magnetism, Ecole Polytechnique Fédérale de Lausanne (EPFL), CH-1015 Lausanne, Switzerland*
[7]*Department of Physics, University of Liverpool, Crown Street, Liverpool L69 7ZE, United Kingdom*
[8]*Laboratory for Developments and Methods, Paul Scherrer Institute, CH-5232 Villigen, Switzerland*
[9]*II. Physikalisches Institut, Universität zu Köln, Zülpicher Strasse 77, D-50937 Köln, Germany*
[10]*DPMC-MaNEP, University of Geneva, CH-1211 Geneva 4, Switzerland*
[11]*Ames Laboratory, U.S. DOE, Iowa State University, Ames, Iowa 50011, USA*
[12]*Department of Physics and Astronomy, Iowa State University, Ames, Iowa 50011, USA*
[13]*Department of Physics, Royal Holloway, University of London, Egham, Surrey TW20 0EX, United Kingdom*

(Received 3 September 2014; revised manuscript received 19 February 2015; published 13 April 2015)

We report on combined neutron and resonant x-ray scattering results, identifying the nature of the spin-orbital ground state and magnetic excitations in $LuVO_3$ as driven by the orbital parameter. In particular, we distinguish between models based on orbital-Peierls dimerization, taken as a signature of quantum effects in orbitals, and Jahn-Teller distortions, in favor of the latter. In order to solve this long-standing puzzle, polarized neutron beams were employed as a prerequisite in order to solve details of the magnetic structure, which allowed quantitative intensity analysis of extended magnetic-excitation data sets. The results of this detailed study enabled us to draw definite conclusions about the classical versus quantum behavior of orbitals in this system and to discard the previous claims about quantum effects dominating the orbital physics of $LuVO_3$ and similar systems.

DOI: 10.1103/PhysRevB.91.161104 PACS number(s): 75.70.Tj, 75.10.Dg, 78.70.Nx, 78.70.Ck

Geometrically frustrated magnetism with its crucial role of quantum effects in purely spin systems is a well-established field with new, exotic phases emerging [1]. Can we, however, have a similar situation in a completely different context, namely, in orbital physics? A positive answer to this question would open up a different field and define another *class of materials*.

The possible role of quantum fluctuations in orbital physics is a very interesting and important question. For small objects such as Jahn-Teller (JT)-active molecules or isolated JT impurities in solids, such quantum effects are well known and constitute a big field of vibronic effects in JT physics [2,3]. On the other hand, in concentrated solids we practically always ignore these effects and treat orbitals (quasi)classically. Therefore, all the more exciting were the suggestions [4,5] that orbitals may behave as essentially quantum objects, in particular, in some perovskite vanadates [6,7], up to the formation of orbital singlets in YVO_3 [7]. If true, it would have opened a large class of phenomena and group materials with quite nontrivial properties.

However, there are also arguments [8,9] that the situation with quantum effects in orbitals may be not so simple and not exactly analogous to that in spin systems. It is predominantly connected with the intrinsically strong orbital-lattice coupling, as a result of which orbital degrees of freedom become "heavy," essentially classical (or one needs to treat also lattice vibrations quantum mechanically, as is done in vibronic physics). Specifically, for YVO_3, Fang and Nagaosa [10] proposed an alternative, essentially classical explanation of the experimental findings of [7], thus casting serious doubts on the importance of orbital quantum effects in RVO_3—practically the only real systems for which these effects were claimed to be observed.

To clarify this important issue, we carried out a detailed experimental study of a material of the same group and with similar properties as YVO_3—$LuVO_3$—using polarized neutron and resonant x-ray scattering.

Specifically, the intriguing proposal made for the RVO_3 compounds was the existence of a novel state—an orbital-Peierls dimerization in the c direction [6,7]. This proposal was based on the observation of a gap in the spin-wave spectrum along L, which implied an alternation of exchange interaction between consecutive layers in the c direction. The alternative proposal of Ref. [10] used the more conventional picture of JT distortion and orbital order (OO) alternating between consecutive ab planes. However, both these theories produce virtually identical spin-wave dispersions along the c direction [see Fig. 1(c), the left part where both theories coincide]. The spin-wave behavior of the two competing models can be drastically different, but only for carefully selected reciprocal lattice directions. Our results along the $[0K2]$ direction [Fig. 1(c), the right part] conclusively favor a model based on Jahn-Teller distortions rather than the orbital-Peierls dimerization for RVO_3. Another limiting experimental factor in order to distinguish between these two pictures is the fact that the material exhibits structural, magnetic, and orbital transitions

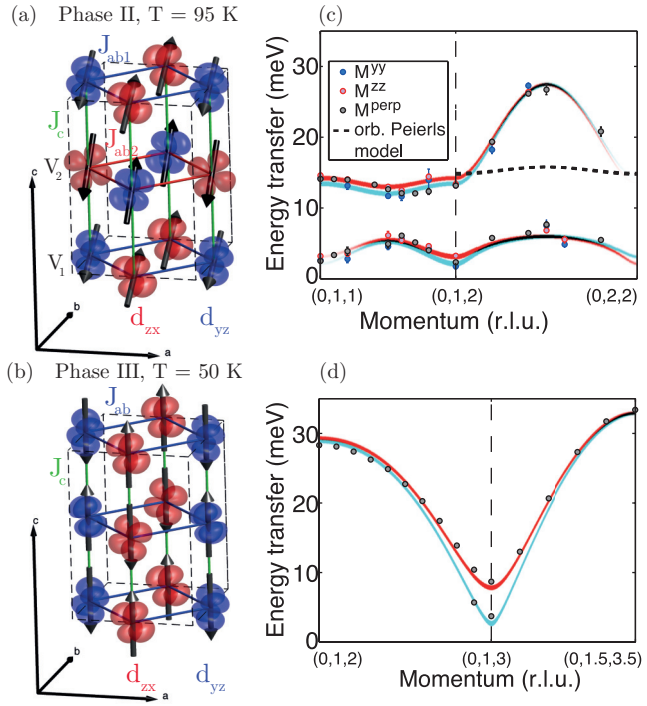

FIG. 1. (Color online) (a), (b) Magnetic ground state configurations, (c), (d) spin waves, and relevant exchange coupling schemes for the two magnetic phases of $LuVO_3$. The magnetic (orbital) structures are derived from neutron polarimetry (resonant x-ray scattering) data while the spin waves were measured using neutron spectroscopy. Calculations shown in (c) are for the Jahn-Teller model (solid lines with linewidth indicating the calculated spectral weight) and orbital-Peierls model (dashed line), as discussed in the text. Colors indicate the different polarization states.

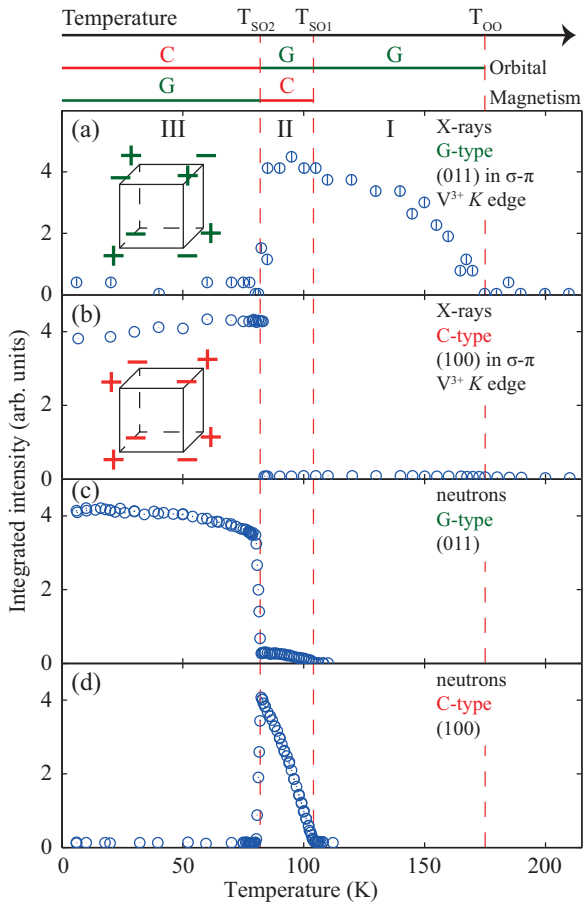

FIG. 2. (Color online) Spin and orbital order parameters of $LuVO_3$ as a function of temperature, revealed by (a), (b) x-ray and (c), (d) neutron scattering. The complementarity of the techniques gives a clear picture of the ordered structures: (a) *G*-type orbital order for phases I, II and (b) *C*-type orbital order for phase III. At the same time, we observe (c) *G*-type spin order for phase III while (d) *C*-type spin order for phase II, in accordance with the Goodenough-Kanamori rules [21]. Note the small *G*-type magnetic component in phase II, which gives an overall canted structure. An overview is schematically drawn on top of the figure. "+" and "−" refer to spins "up" and "down" or an orbital configuration, for instance, "d_{yz}" and "d_{zx}," respectively.

at the same temperature. Therefore, spin-polarized neutron and resonant x-ray beams are essential in order to distinguish between magnetic, orbital, and structural signals. This is of utter importance since a prerequisite to answer the main important question is to first determine the precise magnetic structure. Based on that, one can make a quantitative analysis on the magnetic-excitation intensities of the relevant phase.

$LuVO_3$ is the end member of the RVO_3 family and has the smallest ionic radius, giving rise to increased octahedral distortions. We therefore expect it to be most sensitive to a possible orbital-Peierls dimerization. The V^{3+} ion ($S = 1$) is in an octahedral environment of O atoms (within the perovskite structure) with the two $3d$ electrons occupying t_{2g} orbitals. One electron occupies the xy orbital, and the other occupies one of the two doubly degenerate xz or yz orbitals (or their linear superposition). In $LuVO_3$ the interplay between spin and orbital physics is responsible for the rich phase diagram indicated by bulk measurements [11,12], as for the well-studied YVO_3 [7,13–19]. Upon cooling, $LuVO_3$ first enters an orbitally ordered phase at $T_{OO} = 177$ K (phase I), followed by magnetic ordering at $T_{SO1} = 105$ K (phase II). Below that, yet another orbital-magnetic phase transition takes place, at $T_{SO2} = 82$ K (phase III) [11]. This information, together with the phase numbering used throughout this text, is given in the top of Fig. 2.

Experimental setup details can be found in the Supplemental Material [20]. The resonant x-ray scattering (RXS) experiment, being sensitive to anisotropic properties of the tensorial cross section, yields the charge forbidden Bragg reflections arising from the OO and shown in Figs. 2(a) and 2(b). Specifically, *G*-type orbital ordering is revealed in phases I+II, while *C*-type ordering is found for phase III (schematic diagrams of the order in Fig. 2). *Ab initio* calculations show that electric dipole transitions dominate the cross section in this case. The neutron data shown in Figs. 2(c) and 2(d) complement the x-ray data; they show primarily *C*-type spin ordering for phase II (but with a small admixture of *G* type) and *G*-type spin ordering only for phase III. This combined neutron-RXS result is in agreement with the Goodenough-Kanamori rules (see Ref. [21]).

TABLE I. Exchange parameters for both magnetic phases of $LuVO_3$. The positive sign corresponds to AF coupling.

Phase III (meV)	Phase II (meV)
$J_{ab} = 4.24(21)$	$J_{ab1} = 0.82(3)$
	$J_{ab2} = 5.99(3)$
$J_c = 5.95(19)$	$J_c = -1.29(2)$
$K = [-0.48(12), -0.06(2), 0]$	$K_1 = [0, 0.66(5), 0]$
	$K_2 = [0, 0, 0.66(5)]$

These measurements demonstrate that $LuVO_3$ is an antiferromagnet (AF) with $\boldsymbol{k} = 0$. This, combined with structural phase transitions occurring at the magnetic ordering temperatures, necessitates the use of polarized neutrons to determine the magnetic structures in detail. Spherical neutron polarimetry is used to measure polarization matrices for selected reflections in both magnetic phases, as discussed in the Supplemental Material [20]. The unpolarized intensity data (E5) were used for a cross-check as well as for normalizing the moment size.

Phase III has a collinear G-type magnetic structure as plotted in Fig. 1(b), consistent with the $Pbnm$ orthorhombic space group. The magnetic moments are pointing purely along the crystallographic C axis. For phase II, beam depolarization arising due to orientation domains implies that the space group can no longer be $Pbnm$. Furthermore, in order to have G-type orbital ordering, as observed from our resonant x-ray data, it is necessary to lose the mirror plane perpendicular to the c axis, also inconsistent with $Pbnm$. We could thus fit our data with the lower monoclinic $P2_1/b$ space group and a canted magnetic structure, as shown in Fig. 1(a).

In order to gain deeper insight into structural details affecting the precise environment of the V^{3+} ions, high-resolution powder x-ray diffraction experiments were performed (see the Supplemental Material [20] for details). The orbitals plotted in Fig. 1 follow precisely the octahedral tilts and distortions as determined from refinements of these high-resolution x-ray data.

The spin-wave dispersion was measured in both phases to help model the microscopic Hamiltonian. Polarized neutrons were used to measure the dispersion in phase II [shown in Fig. 1(c)], in order to disentangle the spin waves from the phonon modes, which show similar dispersions. Further, we were able to separate magnetic excitations with different polarization states (M^{yy} and M^{zz}, standard Blume-Maleev coordinate system notation [22]), which is important in the subsequent analysis. Magnons in phase III were measured by unpolarized neutron spectroscopy.

The spin-wave dispersion was modeled using linear spin-wave theory (LSWT) and the SpinW library [23] with a simple Hamiltonian of the form $H = \Sigma_{\langle i,j\rangle} J_{ij}\mathbf{S}_i\mathbf{S}_j + H_{\text{an}}$, where H_{an} is the usual easy-axis single-site anisotropy term as $-KS_z^2$, but with the local easy axes different for different sites (see below). J_{ij} exchange parameters are shown in Fig. 1 (positive J_{ij} denotes AF coupling). Phase III is fitted with two Heisenberg exchange parameters and a single-ion anisotropy term (the parameters given in Table I), yielding a perfect agreement with our data, as shown in Fig. 1(d). The single-ion anisotropy term gives rise to two split modes as well as the overall gap of the system, found to be $E_{\text{gap}} = 3.7(1)$ meV. The situation is more complex and very different for the intermediate temperature phase II. Magnons are observed at both $Q = (012)$ and $Q = (011)$ due to the canted structure ($C + G$ types). This phase is gapped, with four modes and a splitting of ≈5 meV between the two sets of branches. The c-axis energy scale is reduced by more than a factor of 2 while the doubling of the number of modes is in accordance with two inequivalent V sites (lowering of the space group).

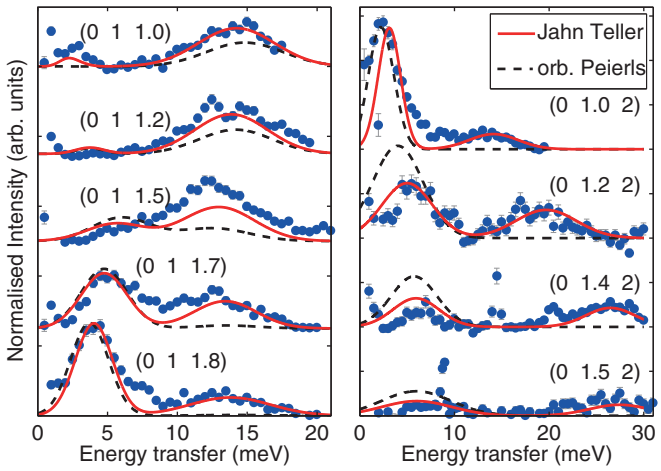

FIG. 3. (Color online) Magnetic scattering intensity as measured in the intermediate phase of $LuVO_3$ ($T = 95$ K). The directions shown are the c^* and b^* axes (left and right panels, respectively). The exchange models being compared are either the 3D Jahn-Teller model (solid red lines) or the orbital-Peierls model (dotted black lines).

In order to determine the Hamiltonian, in this more complex case, it is necessary to model data along a further direction [b axis, Fig. 1(c)]. The dispersion along the b axis rises to 27 meV, an energy which can only be explained by assuming the interaction scheme of Fig. 1(a) with two distinct ab plane couplings alternating along c, as well as a ferromagnetic coupling along the c axis [10]. The parameters of this Hamiltonian which fit the data very precisely are also given in Table I. In order to account for the canting of the moments, two individual directions were assumed for the single-ion anisotropy term: easy b and c axes for V_1 and V_2, respectively, located in alternating ab planes in accordance with the $P2_1/b$ space group symmetry and the interaction scheme. Note that this model accounts not only for the measured spin-wave energies and intensities, but also correctly indexes the M^{yy}/M^{zz} polarization states and further respects the magnetic structure as well as the symmetry of the $P2_1/b$ space group. An alternative orbital-Peierls model with alternating exchange along the c direction and a single coupling in the ab plane would require a lowering of the space group due to loss of a mirror plane along the crystallographic c axis. This model [7] was fitted to the energies of our data set, but predicts an almost flat mode at 15 meV for the dispersion along the b axis [see the black dashed line in Fig. 1(c)] with zero intensity, contrary to our observation. The direct comparison of both models with the data (Fig. 3) shows that indeed the coupling scheme of Fig. 1(a) (continuous red lines)

is in excellent agreement with our data. In contrast, the orbital-Peierls model with exchange couplings alternating along c (dashed black lines) shows large overall discrepancies in the spectral weight distributions. The figure shows the calculated intensities after fitting the dispersion energies (Fig. 1) with a single scaling factor. Note that the symmetry of the monoclinic $P2_1/b$ space group is consistent with inequivalence of the bonds in alternate ab planes [the three-dimensional (3D) JT model], but incompatible with inequivalence of the c-axis bonds between these planes (orbital-Peierls scenario). This is, in addition, a very strong symmetry argument in favor of the former model.

Comparing phase III of $LuVO_3$ at low temperature with YVO_3, we find a direct agreement between the ground state and model Hamiltonian as discussed in Ref. [7]. The moment direction, inelastic gap size, and bandwidth match well. The main difference is a 30% smaller ordered moment and variations of up to 40% in the exchange couplings and anisotropy parameters which can be attributed to the details of lattice distortions and exchange pathways in each case. However, the experimentally determined magnetic structure of phase II at intermediate temperature differs from all other RVO_3 members [7,13,24,25]. The use of polarized neutron diffraction enables precise determination of the moment direction (bc plane) due to the $\boldsymbol{k} = 0$ magnetic propagation vector combined with structural distortions across the magnetic phase transitions. Furthermore, by using a full polarization analysis it is possible to predict the subtle lowering of the space group from orthorhombic to monoclinic, based on symmetry arguments and the observation of orientation domains.

By employing polarized neutron spectroscopy and, in particular, by making extended measurements in two inequivalent directions in reciprocal space, we were able to distinguish between model Hamiltonians in which either the exchange J_{ab} or J_c alternate along the c axis between two values [see Figs. 1(a), 1(c), and 3]. The clear evidence for the first model (J_{ab} alternation) is the superiority of dispersion and intensity fits to this model, compared to the other (J_c alternation). On top, this is in excellent agreement with *ab initio* theoretical calculations given in Ref. [10]. The alternate J_{ab} exchange parameters calculated for YVO_3 are 0.8 and 5.3 meV, and our fitted results for $LuVO_3$ are 0.8 and 6 meV, strongly supporting our conclusion. These first-principle calculations [10] are based on the precise experimentally determined JT distortions of YVO_3 and related vanadates [14–16,26] which do indeed alternate between adjacent ab planes, exactly in the same fashion as J_{ab} in our Hamiltonian. The J_{ab} exchange parameter is very sensitive to these JT distortions and orbital ordering, because it depends on subtle competition between various exchange processes [10]. This explains the large difference between the two alternating values of J_{ab}.

Based on these findings, we conclude that the orbital fluctuations—which are inherent to these systems—are in fact suppressed by the JT distortions. In $LuVO_3$ this results in an overall 3D spin-orbital structure, rather than a quasi-1D orbital dimerized chain.

Summarizing, we have carried out a detailed analysis of the interplay among spin, orbital, and lattice degrees of freedom in the Mott insulator $LuVO_3$. By combining a variety of experimental methods, we are able to uniquely determine the magnetic and orbital states and to model the spin Hamiltonian in the two magnetic phases. These results show that the features, attributed previously to an orbital-Peierls state ("orbital-singlet," similar to spin-singlet dimers) which could have appeared due to quantum effects in orbitals, are in fact a consequence of the static orbital ordering and corresponding Jahn-Teller distortion. Yet, we cannot rule out that the orbital quantum fluctuations may still be present in some form, maybe in different materials. This question deserves further study.

We are grateful to G. Khaliullin, O. Zaharko, Ch. Pfleiderer, and S. Ward for invaluable discussions. We thank the sample environment teams at PSI, ILL, and HZB, where these measurements were performed, for their expert assistance. The research leading to these results has received funding from the European Community's Seventh Framework Programme (FP7/2007-2013) under Grant Agreement No. 290605 (PSI-FELLOW/COFUND). The work of D.I.K. was supported by the German program FOR 1346 and by the Cologne University via German Excellence Initiative. Work at Ames Laboratory was supported by the U.S. Department of Energy (DOE), Office of Science, Basic Energy Sciences, Materials Science and Engineering Division under Contract No. DE-AC02-07CH11358. Use of the Advanced Photon Source, an Office of Science User Facility, is operated for the U.S. DOE by Argonne National Laboratory under Contract No. DE-AC02-06CH11357. X-ray powder diffraction (XRPD) data were collected at the X04SA-MS beamline of the SLS synchrotron at PSI.

[1] *Introduction to Frustrated Magnetism*, edited by C. Lacroix, Ph. Mendels, and F. Mila, Springer Series in Solid-State Sciences Vol. 164 (Springer, Berlin, 2011).

[2] R. Englman, *The Jahn-Teller Effect in Molecules and Crystals* (Wiley, New York, 1972).

[3] I. B. Bersuker, *The Jahn-Teller Effect* (Cambridge University Press, Cambridge, U.K., 2006).

[4] G. Khaliullin and S. Maekawa, Phys. Rev. Lett. **85**, 3950 (2000).

[5] G. Khaliullin, Phys. Rev. B **64**, 212405 (2001).

[6] J. Sirker and G. Khaliullin, Phys. Rev. B **67**, 100408(R) (2003)

[7] C. Ulrich, G. Khaliullin, J. Sirker, M. Reehuis, M. Ohl, S. Miyasaka, Y. Tokura, and B. Keimer, Phys. Rev. Lett. **91**, 257202 (2003).

[8] D. I. Khomskii and M. V. Mostovoy, J. Phys. A: Math. Gen. **36**, 9197 (2003).

[9] D. I. Khomskii, Phys. Scr. **72**, CC8 (2005).

[10] Z. Fang and N. Nagaosa, Phys. Rev. Lett. **93**, 176404 (2004).

[11] S. Miyasaka, Y. Okimoto, M. Iwama, and Y. Tokura, Phys. Rev. B **68**, 100406(R) (2003).

[12] J. Fujioka, T. Yasue, S. Miyasaka, Y. Yamasaki, T. Arima, H. Sagayama, T. Inami, K. Ishii, and Y. Tokura, Phys. Rev. B **82**, 144425 (2010).

[13] M. Reehuis, C. Ulrich, P. Pattison, B. Ouladdiaf, M. C. Rheinstädter, M. Ohl, L. P. Regnault, M. Miyasaka, Y. Tokura, and B. Keimer, Phys. Rev. B **73**, 094440 (2006).

[14] G. R. Blake, T. T. M. Palstra, Y. Ren, A. A. Nugroho, and A. A. Menovsky, Phys. Rev. Lett. **87**, 245501 (2001).
[15] G. R. Blake, T. T. M. Palstra, Y. Ren, A. A. Nugroho, and A. A. Menovsky, Phys. Rev. B **65**, 174112 (2002).
[16] M. Noguchi, A. Nakazawa, S. Oka, T. Arima, Y. Wakabayashi, H. Nakao, and Y. Murakami, Phys. Rev. B **62**, R9271(R) (2000).
[17] Y. Ren, T. T. M. Palstra, D. I. Khomskii *et al.*, Nature (London) **396**, 441 (1998).
[18] Y. Ren, T. T. M. Palstra, D. I. Khomskii, A. A. Nugroho, A. A. Menovsky, and G. A. Sawatzky, Phys. Rev. B **62**, 6577 (2000).
[19] D. Bizen, N. Shirane *et al.*, J. Phys.: Conf. Ser. **150**, 042010 (2009).
[20] See Supplemental Material at http://link.aps.org/supplemental/10.1103/PhysRevB.91.161104 for experimental setups, nuclear and magnetic structural details.
[21] D. I. Khomskii, *Transition Metal Compounds* (Cambridge University Press, Cambridge, U.K., 2014).
[22] M. Blume, Phys. Rev. **130**, 1670 (1963).
[23] S. Toth and B. Lake, arXiv:1402.6069.
[24] A. Muñoz, J. A. Alonso *et al.*, Chem. Mater. **16**, 1544 (2004).
[25] M. Reehuis, C. Ulrich, K. Prokeš, S. Matas, J. Fujioka, S. Miyasaka, Y. Tokura, and B. Keimer, Phys. Rev. B **83**, 064404 (2011).
[26] P. Bordet, C. Chaillout *et al.*, J. Solid State Chem. **106**, 253 (1993).